Energy 55 (2013) 899–904

Contents lists available at SciVerse ScienceDirect

Energy

journal homepage: www.elsevier.com/locate/energy

Thermodynamic irreversibility and performance characteristics of thermoelectric power generator

Ahmet Z. Sahin*, Bekir S. Yilbas

Mechanical Engineering Department, King Fahd University of Petroleum and Minerals, Dhahran 31261, Saudi Arabia

ARTICLE INFO

Article history:
Received 3 December 2012
Received in revised form
13 March 2013
Accepted 14 March 2013
Available online 17 April 2013

Keywords:
Thermoelectric generator
Performance
Entropy generation

ABSTRACT

Thermodynamic irreversibility and performance characteristics of a thermoelectric power generator are investigated. The influence of the external load parameter, the thermal conductivity ratio, the figure of Merit, and the conductance ratio on the efficiency, the output power, and the entropy generation rate is predicted for various device operating parameters. It is found that the device efficiency increases to reach its maximum at the critical value of the output power and operating the device beyond the critical output power lowers the thermal efficiency and enhances the entropy generation rate significantly in the device.

1. Introduction

Thermoelectric generators are one of the potential candidates for renewable energy conversion. Although their efficiency is low, their environment friendly nature, simple design, and operation are the driving forces for the current research interest of these devices. The recent developments in thermoelectric materials improve notably the figure of Merit and the device efficiency. However, the performance of the thermoelectric generators can be further improved through minimization of thermodynamic losses during the operation. One of the methods to maximize the thermal efficiency of the thermoelectric device is to minimize the entropy generation rate in the thermoelectric system. Therefore, investigation into entropy generation rate and the performance of the thermoelectric generators becomes essential.

Considerable research studies were carried out to examine thermal characteristics of thermoelectric systems. Optimization study for low-temperature waste heat thermoelectric generator system was carried out by Gou et al. [1]. They demonstrated that expanding heat sink area in a proper range and enhancing cold-side heat transfer capacity, thermoelectric device performance improved notably. Performance of two-stage thermoelectric refrigerator system was studied by Meng et al. [2]. They presented analytical expressions for the electrical current in terms of the cooling load versus the electrical current and the coefficient of performance versus the electrical current of the combined devices. The thermoelectric generator and multi-scale irreversibility were investigated by Meng et al. [3]. They presented the effects of external irreversibility on the performance of the thermoelectric generator. The constructal design of a thermoelectric device was examined by Pramanick and Das [4]. They demonstrated that the maximum permissible length was dependent on applied temperature gradient whereas the minimum allowable length was independent of the temperature gradient. Topping cycle and thermoelectric power generation were studied by Sahin et al. [5]. They showed that for a certain combination of operating and thermoelectric device parameters, thermal efficiency of the topping cycle became slightly higher than that of the same system without the presence of the thermoelectric generators. Thermoelectric device for optimum external load parameter and slenderness ratio for the maximum efficiency was investigated by Yilbas and Sahin [6]. They indicated that for a fixed thermal conductivity ratio, the external load parameter increased with increasing slenderness ratio while the electrical conductivity ratio of the p and n pins reduced in the device. Optimization of thermoelectric generating process was carried out by Garcia and Zorraquino [7]. They presented the future of the cogeneration system incorporating the thermoelectric devices. The integrated assessment of energy conversion processes through thermodynamic, economic, and environmental parameters was carried out by Tonon at al. [8]. They presented detailed analysis to evaluate economic and exergetic behavior of the energy conversion processes including the thermoelectric devices. The analytical model for parallel thermoelectric generator was proposed by Liang et al. [9]. They showed that the thermal contact resistance reduced the output power by reducing the temperature difference between

* Corresponding author.
E-mail address: azsahin@kfupm.edu.sa (A.Z. Sahin).

0360-5442/$ – see front matter © 2013 Elsevier Ltd. All rights reserved.
http://dx.doi.org/10.1016/j.energy.2013.03.064

the two sides of the thermoelectric elements. Solar thermoelectric generator for micro-power applications was investigated by Amatya et al. [10]. They introduced two stage thermoelectric devices for the solar energy conversion. The heat transfer area optimization for a thermoelectric generator was examined by Chen et al. [11]. They optimized the ratio of heat transfer surface area of the high temperature site to the total heat transfer surface area to maximize the power output and the thermal efficiency of the thermoelectric generator. Thermodynamic analysis of a thermoelectric device was carried out by Kassas [12]. His results revealed that the second law efficiency improved with increasing emitter to collector temperature ratio and reduced with increasing collector temperature. Various aspects of thermoelectric devices and their applications were studied in Refs. [3,13–24]. It is observed from the literature search that there is a considerable increase in the research work during the recent years on the thermoelectric power generation. However, it is also observed that only a few of those papers discuss entropy generation in thermoelectric device briefly. Therefore, there is a need for further investigation on the entropy generation and associated irreversibility in the thermoelectric generators.

In the present study, thermodynamic analysis including the maximum efficiency, the maximum output power, and the rate of entropy generation is carried out for a thermoelectric power generator. The device characteristics are examined for various device operating parameters including the external load parameter. The behavior of entropy generation rate for the maximum device output power and the efficiency is presented.

2. Thermal analysis

A schematic view of the thermoelectric power generator is shown in Fig. 1. Heat transfer occurs from a high temperature reservoir at T_H to the lower plate. This constitutes the high and low temperature junctions of the two semiconductors of n-type and p-type. The hot junction of the semiconductors is at temperature T_1. As the heat transfer is conducted from the hot junction to the cold junction at temperature T_2, electric current is generated. The electrical current that flows through the semiconductors depends on the thermoelectric characteristics of the semiconductors such as the Seebeck coefficient and the electrical conductance causes joule heating in both semiconductors. The heat transfers crossing the upper hot junction and the lover cold junction are given, respectively, as:

$$\dot{Q}_H = \alpha I T_1 + K(T_1 - T_2) - \frac{1}{2} I^2 R \tag{1}$$

and

$$\dot{Q}_L = \alpha I T_2 + K(T_1 - T_2) + \frac{1}{2} I^2 R \tag{2}$$

where

$$\alpha = \alpha_p - \alpha_n, \quad K = \frac{A_p k_p}{L_p} + \frac{A_n k_n}{L_n}, \quad R = \frac{L_p}{A_p k_{e,p}} + \frac{L_n}{A_n k_{e,n}}.$$

Considering the heat conductances between the high and cold temperature reservoirs, the heat transfer rates from the hot and cold junctions, respectively, are given as:

$$\dot{Q}_H = C_H(T_H - T_1) \tag{3}$$

and

$$\dot{Q}_L = C_L(T_2 - T_L). \tag{4}$$

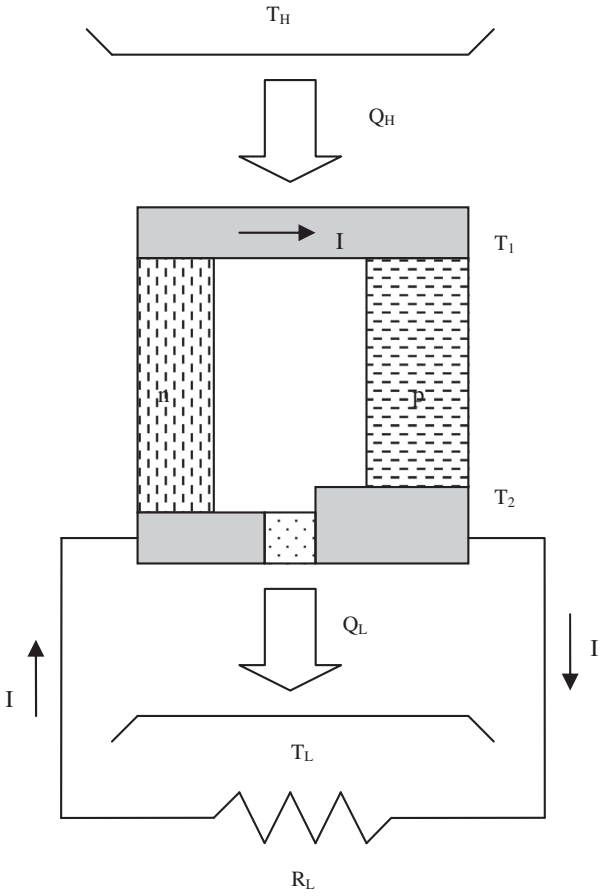

Fig. 1. Schematic view of the thermoelectric power generator.

The electrical current generated as a result of the temperature difference between the hot and cold junctions is proportional to the Seebeck effect and inversely proportional with the total electrical resistance of the circuit i.e.

$$I = \frac{\alpha(T_1 - T_2)}{R_L + R} \tag{5}$$

The useful power generated as a result of electrical current can be written as:

$$\dot{W}_{\text{out}} = \dot{Q}_H - \dot{Q}_L = \alpha I(T_1 - T_2) - I^2 R = I^2 R_L. \tag{6}$$

On the other hand, the efficiency of the thermoelectric generator is given by:

$$\eta = \frac{\dot{W}_{\text{out}}}{\dot{Q}_H}. \tag{7}$$

In cases where the heat transfers occur between the semiconductors junctions and the high and low temperature reservoirs, the thermal conductances determine the hot and cold junction temperatures. In turn, the generated electrical current and the efficiency are related to the thermal conductances as well as the other thermoelectric parameters mentioned above.

From equations (1) and (3), the hot and cold junction temperatures can be related to the thermal conductance C_H and the temperature of the high temperature reservoir T_H, i.e:

$$\frac{\alpha^2(T_1-T_2)T_1}{R_L+R}+K(T_1-T_2)-\frac{1}{2}\frac{\alpha^2(T_1-T_2)^2}{(R_L+R)^2}R=C_H(T_H-T_1) \quad (8)$$

Equation (8) can be made dimensionless by defining:

$$Z=\frac{\alpha^2}{KR} \quad \rho=\frac{R_L}{R} \quad \lambda=\frac{K}{C_H} \quad \theta_1=\frac{T_1}{T_H} \quad \theta_2=\frac{T_2}{T_H}$$

So that the dimensionless form becomes:

$$\frac{ZT_H\lambda(\theta_1-\theta_2)\theta_1}{\rho+1}+\lambda(\theta_1-\theta_2)-\frac{1}{2}\frac{ZT_H\lambda(\theta_1-\theta_2)^2}{(\rho+1)^2}=1-\theta_1 \quad (9)$$

Similarly, using equations (2) and (4) another relationship between the junction temperatures is obtained as:

$$\frac{\alpha^2(T_1-T_2)T_2}{R_L+R}+K(T_1-T_2)+\frac{1}{2}\frac{\alpha^2(T_1-T_2)^2}{(R_L+R)^2}R=C_L(T_2-T_L) \quad (10)$$

Defining two new dimensionless parameters:

$$\sigma=\frac{C_L}{C_H} \quad \theta_L=\frac{T_L}{T_H}$$

equation (10) becomes:

$$\frac{ZT_H\lambda(\theta_1-\theta_2)\theta_2}{\rho+1}+\lambda(\theta_1-\theta_2)+\frac{1}{2}\frac{ZT_H\lambda(\theta_1-\theta_2)^2}{(\rho+1)^2}=\sigma(\theta_2-\theta_L). \quad (11)$$

Equations (9) and (11) can be solved simultaneously for the dimensionless hot and cold junction temperatures, θ_1 and θ_2, respectively.

The dimensionless power generation is:

$$\frac{W}{KT_H}=\frac{(\theta_1-\theta_2)^2\rho}{(\rho+1)^2}ZT_H \quad (12)$$

and the efficiency is:

$$\eta=\frac{(\theta_1-\theta_2)^2\rho\lambda ZT_H}{(\rho+1)^2(1-\theta_1)}. \quad (13)$$

2.1. Entropy generation rate in thermoelectric device

Entropy generation rate in the thermoelectric device is due to both internal and external heat transfer mechanisms. The total entropy generation rate can be written as:

$$\dot{S}_{\text{gen}}=\dot{Q}_H\left(\frac{T_H-T_1}{T_HT_1}\right)+\dot{Q}_L\left(\frac{T_2-T_L}{T_2T_L}\right)-\frac{\dot{Q}_H}{T_1}+\frac{\dot{Q}_L}{T_2} \quad (14)$$

The first two terms on the right hand side of equation (14) represent the entropy generation rate due to the heat transfer from the high temperature reservoir to the hot junction of the thermoelectric device and that from the cold junction of the thermoelectric device to the low temperature reservoir, respectively. On the other hand, the last two terms on the right hand side of equation (14) stand for the internal entropy generation rate that take place in the thermoelectric device. It can be shown that equation (14) simplifies to

$$\dot{S}_{\text{gen}}=-\frac{\dot{Q}_H}{T_H}+\frac{\dot{Q}_L}{T_L} \quad (15)$$

Using equations (3) and (4), the total entropy generation rate becomes:

$$\dot{S}_{\text{gen}}=-C_H\left(1-\frac{T_1}{T_H}\right)+C_L\left(\frac{T_2}{T_L}-1\right) \quad (16)$$

The entropy generation rate can be made dimensionless in the form:

$$S^*=\frac{\dot{S}_{\text{gen}}}{C_H}=-(1-\theta_1)+\sigma\left(\frac{\theta_2}{\theta_L}-1\right) \quad (17)$$

The following figures show the effect of the foregoing dimensionless parameters on the power generation, efficiency and entropy generation rate.

3. Results and discussion

Thermodynamic analysis including the maximum power, the maximum efficiency, and the entropy generation rate for the thermoelectric device is carried out and the device performance characteristics are analyzed for various operating conditions.

Fig. 2 shows the dimensionless device output power, the efficiency and the dimensionless entropy generation rate with the external load parameter (ρ). The device efficiency and the output power increase with the external load parameter, and the entropy generation rate reduces with increasing external load parameter. It should be noted that the external load parameter is the ratio of the external resistance to the device overall resistance. Increasing external load parameter enhances both the thermal efficiency and the output power (equations (12) and (13)). However, further increase in the external load parameter reduces the efficiency and the output power of the device. This indicates that operating the device for larger external resistance as compared to the device overall resistance, the current derived from the device is not high enough to secure high output power and consequently high efficiency. In addition, large differences in impedances due to the device and external resistances have adverse effect on the device performance (i.e. both the efficiency and the power output from the thermoelectric device decrease). Although the thermodynamic irreversibility in the thermoelectric device due to entropy generation reduces because of reduced entropy generation rate, the capacity of the device is not fully utilized efficiently for high external load parameters.

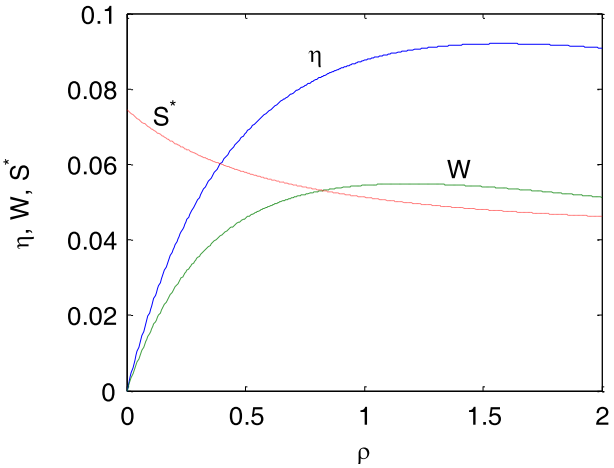

Fig. 2. The effect of the dimensionless external load on the dimensionless power, the efficiency and the entropy generation rate ($\lambda=0.1$, $\theta_L=0.5$, $ZT_H=1.5$, $\sigma=1.0$).

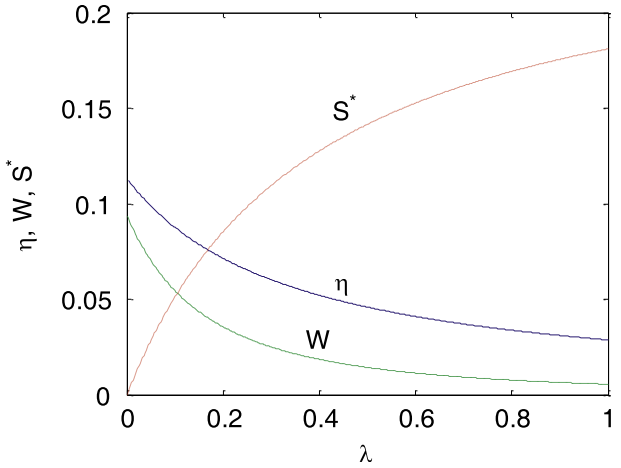

Fig. 3. The effect of the dimensionless thermal conductivity on the dimensionless power, the efficiency and the entropy generation rate ($\rho = 1.0$, $\theta_L = 0.5$, $ZT_H = 1.5$, $\sigma = 1.0$).

Fig. 3 shows the device output power, the efficiency, and the entropy generation rate with the thermal conductivity ratio. Increasing thermal conductivity ratio increases the heat conduction from the high temperature plate to the low temperature plate (across the device) while enhancing the entropy generation rate. In addition, increased device thermal conductivity lowers the thermoelectric efficiency due to high rate of heat rejection without contributing to the power generation. Moreover, the reduction in output power and efficiency is sharp for thermal conductivity ratio $\lambda \leq 0.5$ and the reduction becomes gradual with increasing thermal conductivity ratio. This is more pronounced for device output power; in which case, almost 50% of the output power is lost when thermal conductivity ratio becomes 0.1. Therefore, small increase in thermal conductivity ratio has detrimental effect on the efficiency and the output power for $0 \leq \lambda \leq 0.5$. Entropy generation rate increases gradually for $0.5 \leq \lambda \leq 1.0$ and this increase becomes high for $0 \leq \lambda \leq 0.5$.

Fig. 4 shows the device output power, the efficiency, and the entropy generation rate with the figure of Merit. The efficiency, the output power and the entropy generation rate increase with the figure of Merit. The increase in the efficiency and the output power is considerably higher than the entropy generation rate since the entropy generation rate is a function of the heat input and the heat rejected from the device (equation (14)), increasing output power

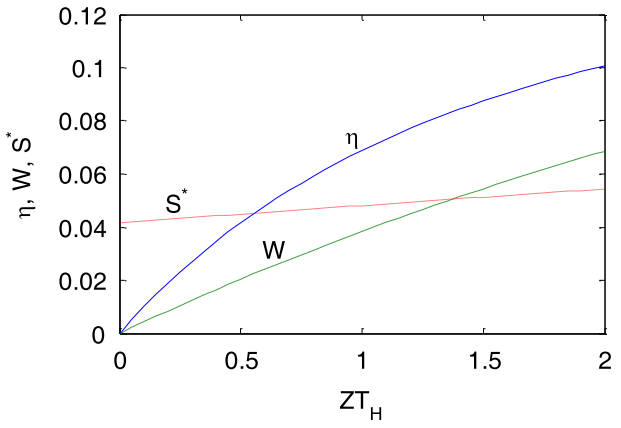

Fig. 4. The effect of the figure of Merit on the dimensionless power, the efficiency and the entropy generation rate ($\rho = 1.0$, $\lambda = 0.1$, $\theta_L = 0.5$, $\sigma = 1.0$).

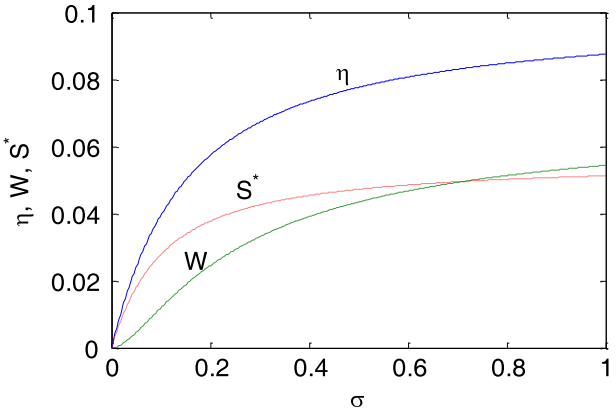

Fig. 5. The effect of the conductance ratio on the dimensionless power, the efficiency and the entropy generation rate ($\rho = 1.0$, $\lambda = 0.1$, $\theta_L = 0.5$, $ZT_H = 1.5$).

requires high heat input and low heat rejection from the device. In addition, the figure of Merit influences significantly the output power and the efficiency (equations (11) and (12)); therefore, improving output power inherently enhances the entropy generation rate in the device. The amount of heat leakage, due to conduction across the device increases slightly with increase of the figure of Merit. In this case, the entropy generation rate due to slight heat transfer enhancement increases gradually the entropy generation rate.

Fig. 5 shows the device output power, the efficiency and the entropy generation rate with the conductance ratio. The efficiency and the output power as well as the entropy generation rate increase with increasing conductance ratio. It should be noted that the conductance ratio ($\sigma = C_L/C_H$) is associated with the heat input and the heat rejected across the device (equations (3) and (4)). However, the rise of the efficiency, the output power and the entropy generation rate is sharper for $\sigma \leq 0.3$. As the conductance ratio increases further, this rise becomes gradual. The entropy generation rate indicates that the thermodynamic irreversibility for low values of the ratio rises sharply, despite the efficiency of the device rises sharply. Since the device efficiency is on the order of 4% for this low level of conductance ratio, heat transfer from the high temperature source does not yield high rate of useful energy to attain high efficiencies. Consequently, operating the device at low conductance ratio is not beneficial in terms of efficiency. Moreover,

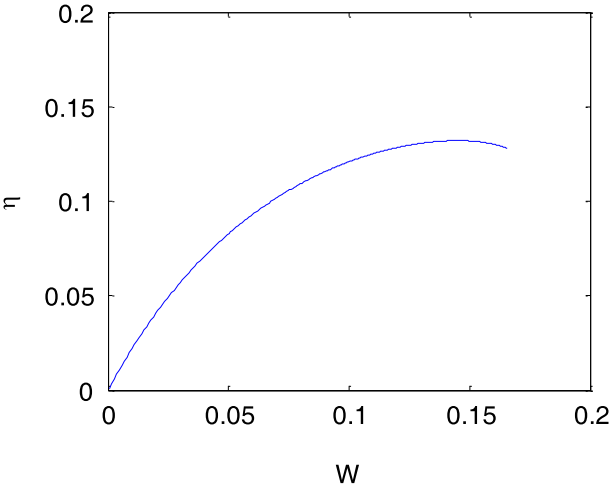

Fig. 6. Efficiency versus the dimensionless power for varying figure of Merit, $ZT_H = 0$–10 ($\rho = 1.0$, $\lambda = 0.1$, $\theta_L = 0.5$, $\sigma = 1.0$).

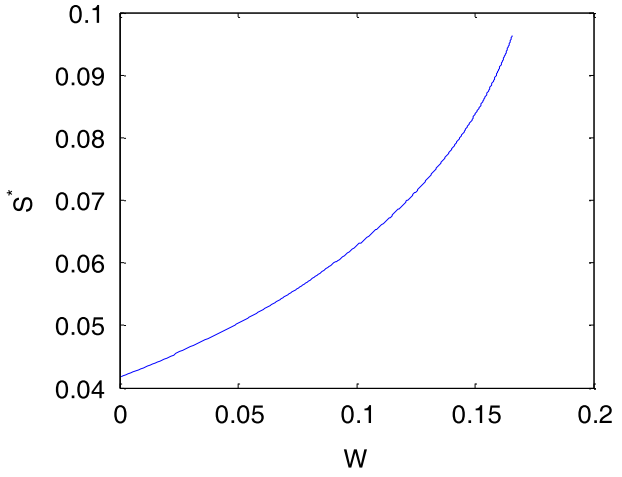

Fig. 7. Dimensionless entropy generation rate versus the dimensionless power for varying figure of Merit, $ZT_H = 0–10$. ($\rho = 1.0$, $\lambda = 0.1$, $\theta_L = 0.5$, $\sigma = 1.0$).

increasing the conductance ratio increases the output power, the efficiency, and gradual increase in the entropy generation rate. Therefore, the device with high conduction ratio has better performance characteristics than that corresponding to the low conductance ratio.

Fig. 6 shows variation of the device efficiency with the output power while Figs. 7 and 8 show the entropy generation rate with the output power and the efficiency, respectively. The efficiency increases to reach its maximum with increasing the output power. This indicates that the device efficiency continuously increases to its maximum with increasing output power. Moreover, further increase in the output power beyond the maximum efficiency, the device efficiency reduces sharply. However, further reduction in the device efficiency results in slightly reduced output power. Consequently, operating the device at low output power causes reduced efficiency and operating at high output power lowers the efficiency. Consequently, operating the device at output power corresponding to the maximum efficiency should be desirable. In the case of the entropy generation rate with the output power (Fig. 7), the rate of entropy generation increases gradually with increasing output power; however, further increase in the output power result in sharp rise of the entropy generation rate. This indicates that the thermodynamic irreversibility increases considerably as the output

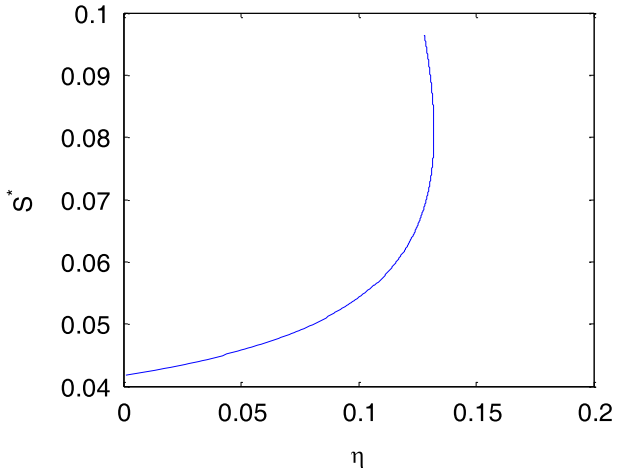

Fig. 8. Dimensionless entropy generation rate versus the efficiency for varying figure of Merit, $ZT_H = 0–10$. ($\rho = 1.0$, $\lambda = 0.1$, $\theta_L = 0.5$, $\sigma = 1.0$).

power increases beyond the critical value. The similar behavior is also observed from the efficiency curve. Consequently, operating device beyond the maximum efficiency causes significant increase in the entropy generation rate while lowering the device performance. Although slight increase in the output power beyond its critical value reduces the efficiency slightly, the thermodynamic irreversibility increases notably. To reduce the thermodynamic irreversibility and increase the efficiency, device should be operated up to its critical value of the output power.

4. Conclusions

The thermoelectric device characteristics are investigated for optimal operating conditions and the thermodynamic irreversibility as measured by the entropy generation rate is examined for different design and operating parameters. The influence of the external load parameter, the thermal conductivity ratio, the figure of Merit, and the conductance ratio on the device output power, the efficiency, and the entropy generation rate are predicted. The relation between the maximum efficiency and the output power is established and the rate of entropy generation with the operating condition is investigated. It is found that increasing external load parameter enhances the efficiency, the output power while lowering the entropy rate generation in the device. Increasing the thermal conductivity ratio lowers the efficiency and the output power, and increases the entropy generation rate. This behavior is due to increased heat transfer rate across the device. Improving the figure of Merit increases the efficiency, the output power, and the entropy generation rate, provided that the entropy generation rate increases gradually with increasing figure of Merit. Increasing conductance ratio increases the efficiency, the output power and the entropy generation rate, provided that increase of device characteristics at low values of the conduction ratio is sharp. The efficiency of the device increases to reach its maximum value with increasing output power and as the output power increases further, it reduces. This is associated with the sharp increase in the thermodynamic irreversibility beyond the critical value of the work done. Therefore, the entropy generation rate increases sharply with increasing device output power beyond its critical value. Further increase in the entropy generation rate lowers both the device output power and the efficiency. Consequently, operating the device within the range of its critical value of the parameters results in the highest efficiency and the reasonably low entropy generation rate across the device.

Acknowledgments

The authors acknowledge the funded project RG 1204 via support of Thermoelectric Group formed by the Deanship of Scientific Research and Center of Excellence for Scientific Research Collaboration with MIT and King Fahd University of Petroleum and Minerals, Dhahran, Saudi Arabia for this work.

Nomenclature

A_n	cross sectional area of n-type semiconductor, (m^2)
A_p	cross sectional are of p-type semiconductor, (m^2)
C_H	thermal conductance at high temperature reservoir, (W/K)
C_L	thermal conductance at low temperature reservoir, (W/K)
I	electrical current, (A)
$k_{e,n}$	electrical conductivity of n-type semiconductor, (1/Ωm)
$k_{e,p}$	electrical conductivity of p-type semiconductor, (1/Ωm)
k_n	thermal conductivity of n-type semiconductor, (W/mK)
k_p	thermal conductivity of p-type semiconductor, (W/mK)

K	overall thermal conductivity of the thermoelectric generator, $K = (A_p k_p/L_p) + (A_n k_n/L_n)$, (W/K)
L_n	length of n-type semiconductor, (m)
L_p	length of p-type semiconductor, (m)
R	overall electrical resistivity of the thermoelectric generator, $R = (L_p/A_p k_{e,p}) + (L_n/A_n k_{e,n})$, (Ω)
R_L	external electrical load, (Ω)
$\dot{S}_{\text{gen}}$	total rate of entropy generation, (W/K)
S^*	dimensionless entropy generation rate, $S^* = \dot{S}_{\text{gen}}/(\dot{Q}_H/T_H)$
T_1	hot side temperature of the thermoelectric generator, (K)
T_2	cold side temperature of the thermoelectric generator, (K)
T_H	temperature of hot reservoir, (K)
T_L	temperature of cold reservoir, (K)
$\dot{Q}_L$	heat flux at cold side, (W)
$\dot{Q}_H$	heat flux at hot side, (W)
$\dot{W}_{\text{out}}$	power output from the thermoelectric generator, (W)
Z	figure of Merit, $Z = \alpha^2/KR$, (1/K)
α	total Seebeck coefficient, $\alpha = \alpha_p - \alpha_n$, (V/K)
α_p	Seebeck coefficient of the p-type semiconductor, (V/K)
α_n	Seebeck coefficient of the n-type semiconductor, (V/K)
λ	dimensionless thermal conductivity, $\lambda = K/C_H$
η	efficiency
ρ	dimensionless external load, $\rho = R_L/R$
σ	conductance ratio, $\sigma = C_L/C_H$
θ_1	dimensionless hot side temperature
θ_2	dimensionless cold side temperature
θ_L	dimensionless cold reservoir temperature

References

[1] Guo X, Xiao H, Yan S. Modeling experimental study and optimization on low-temperature waste heat thermoelectric generator system. Applied Energy 2010;87(10):3131–6.

[2] Meng F, Chen L. Performance optimization for two-stage thermoelectric refrigerator system driven by two-stage thermoelectric generator. Cryogenics 2009;49(2):57–65.

[3] Meng F, Chen L, Sun F. A numerical model and comparative investigation of a thermoelectric generator with multi-irreversibilities. Energy 2011;36(5):3513–22.

[4] Pramancis AK, Das PK. Constructal design of a thermoelectric device. International Journal of Heat and Mass Transfer 2006;49(7–8):1420–9.

[5] Sahin AZ, Yilbas BS, Shuja SZ, Momin O. Investigation into topping cycle: thermal efficiency with and without presence of thermoelectric generator. Energy 2011;36(7):4048–54.

[6] Yilbas BS, Sahin AZ. Thermoelctric device and optimum external load parameter and slenderness ratio. Energy 2010;35(12):5380–4.

[7] Garcia I, Zorraquino JVM. Energy and environmental optimization in thermoelectrical generation processes-application of a carbon dioxide capture system. Energy 2002;27(6):607–23.

[8] Tonon S, Brown MT, Luchi F, Mirandola A, Stoppato A, Ulgiati S. An integrated assessment of energy conversion processes by means of thermodynamic, economic and environmental parameters. Energy 2006;31(1):149–63. SPEC ISS.

[9] Liang G, Zhou J, Huang X. Analytical model of parallel thermoelectric generator. Applied Energy 2011;88(12):5193–9.

[10] Amatya R, Ram RJ. Solar thermoelectric generator for micropower applications. Journal of Electronic Materials 2010;39(9):1735–40.

[11] Chen L, Sun F, Wu C. Thermoelectric-generator with linear phenomenological heat-transfer-law. Applied Energy 2005;81(4):358–64.

[12] Kassas M. Thermodynamic analysis of a thermoelectric device. International Journal of Exergy 2007;4(2):168–79.

[13] Champier D, Bédécarrats JP, Kousksou T, Rivaletto M, Strub F, Pignolet P. Study of a TE (thermoelectric) generator incorporated in a multifunction wood stove. Energy 2011;36(3):1518–26.

[14] Champier D, Bedecarrats JP, Rivaletto M, Strub F. Thermoelectric power generation from biomass cook stoves. Energy 2010;35(2):935–42.

[15] Chen J, Yan Z, Wu L. Nonequilibrium thermodynamic analysis of a thermoelectric device. Energy 1997;22(10):979–85.

[16] Astrain D, Vián JG, Martínez A, Rodríguez A. Study of the influence of heat exchangers' thermal resistances on a thermoelectric generation system. Energy 2010;35(2):602–10.

[17] Chen W, Liao C, Hung C, Huang W. Experimental study on thermoelectric modules for power generation at various operating conditions. Energy 2012;45(1):874–81.

[18] Cheng T, Cheng C, Huang Z, Liao G. Development of an energy-saving module via combination of solar cells and thermoelectric coolers for green building applications. Energy 2011;36(1):133–40.

[19] Hsiao YY, Chang WC, Chen SL. A mathematic model of thermoelectric module with applications on waste heat recovery from automobile engine. Energy 2010;35(3):1447–54.

[20] Rezania A, Rosendahl LA. Thermal effect of a thermoelectric generator on parallel microchannel heat sink. Energy 2012;37(1):220–7.

[21] Wang C, Hung C, Chen W. Design of heat sink for improving the performance of thermoelectric generator using two-stage optimization. Energy 2012;39(1):236–45.

[22] Shu G, Zhao J, Tian H, Liang X, Wei H. Parametric and exergetic analysis of waste heat recovery system based on thermoelectric generator and organic rankine cycle utilizing R123. Energy 2012;45(1):806–16.

[23] Şişman A, Yavuz H. The effect of joule losses on the total efficiency of a thermoelectric power cycle. Energy 1995;20(6):573–6.

[24] Wang X, Huang Y, Cheng C, Ta-Wei Lin D, Kang C. A three-dimensional numerical modeling of thermoelectric device with consideration of coupling of temperature field and electric potential field. Energy 2012;47(1):488–97.